RSC Advances

PAPER

View Article Online
View Journal | View Issue

Cite this: *RSC Adv.*, 2026, **16**, 15392

Umpolung strategy for the electrochemical synthesis of novel anthraquinone-based sulfonamide derivatives: a facile and sustainable strategy

Davood Nematollahi, *[ab] Niloofar Mohamadighader[a] and Faezeh Zivari-Moshfegh[a]

A facile and sustainable galvanostatic strategy was developed for the synthesis of novel sulfonamide derivatives containing anthraquinone moieties. These syntheses were successfully carried out in a divided cell (divided by glass frit) using a graphite anode and a stainless steel cathode in water/acetonitrile solutions at room temperature. The Umpolung strategy employed in these syntheses is straightforward. It is based on the oxidative conversion of 1,4-diaminoanthraquinone from a nucleophile to an electrophile, followed by its reaction with arylsulfinic acid derivatives. The synthesis strategy, as well as the mechanism governing it, has been determined based on the differences in data obtained from electrochemical studies on the oxidation of 1,4-diaminoanthraquinone in the absence and presence of arylsulfinic acid derivatives. This process exhibits high atom economy, does not require a catalyst, is carried out in one pot, is easily scalable, and can be used for a wide range of arylsulfinic acid derivatives.

Received 2nd January 2026
Accepted 25th February 2026

DOI: 10.1039/d6ra00036c

rsc.li/rsc-advances

Introduction

Anthraquinones are a group of compounds classified as quinones and are found in natural materials. These compounds are natural pigments, and approximately 700 of their compounds have been identified.[1] In addition to their well-known use as natural dyes, anthraquinones are of interest to researchers due to their remarkable biological activities, including anti-inflammatory, anticancer, antibacterial, antifungal, antimalarial, diuretic, and antiarthritic properties.[1,2] 1,4-Diaminoanthraquinone (**DAA**) (Fig. 1) is a member of this family that is used as a precursor for dyes and has applications in optical sensors.[3] **DAA** and its derivatives have also been used in the fixation of lactate dehydrogenase.[4]

On the other hand, the benzenesulfonanilide skeleton (Fig. 1) has been identified as a remarkable scaffold in drug discovery. For example, in 1998, a benzenesulfonamide derivative (a hydroxyphenoxybenzenesulfonanilide derivative) was reported by Merck researchers as one of the first selective human β3-AR agonists.[5,6] In 2009, Maruyama *et al.* selected this derivative as their lead compound.[7] In 2007, Zheng *et al.* designed and synthesized simple benzenesulfonanilide-type cyclooxygenase-1-selective inhibitors as analgesic agents without causing gastric damage.[8] In 2012, Rew *et al.* introduced a series of benzenesulfonanilide derivatives as 11b-HSD1 inhibitors.[9] In 2016, Yamada *et al.* introduced *N*-(4-phenoxyphenyl) benzenesulfonamide derivatives as a new class of nonsteroidal progesterone receptor (PR) antagonists.[10] In 2023, Ouellette *et al.* reported that 4-(3-alkyl-2-oxoimidazolidin-1-yl)-*N*-phenylbenzenesulfonamides are prodrugs that are bioactivated by cytochrome P450 1A1 in breast cancer cells to form the potent metabolite 4-(2-oxoimidazolidin-1-yl)-*N*-phenylbenzenesulfonamide.[11]

The interesting and sometimes unique properties of 1,4-diaminoanthraquinone (**DAA**) and benzenesulfonanilide prompted us to synthesize molecules containing both moieties and hope that, like other anthraquinone-based sulfonamide derivatives,[12] they will exhibit significant pharmacological properties. For this purpose, we converted **DAA** into an electron acceptor (Michael) by taking two electrons from it and then reacting it with arylsulfinic acids (**SUL**) as nucleophiles. In this

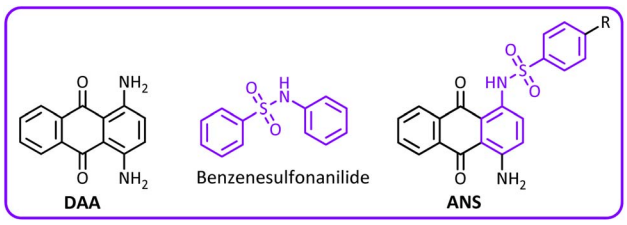

Fig. 1 Structures of 1,4-diaminoanthraquinone (**DAA**), benzenesulfonanilide, and synthesized compounds.

[a]*Faculty of Chemistry and Petroleum Sciences, Bu-Ali Sina University, Hamedan 65178-38683, Iran. E-mail: nemat@basu.ac.ir*

[b]*Plant Chemistry Research Center, Bu-Ali Sina University, Hamedan, Iran*

study, we developed a simple and practical one-pot electrochemical method to obtain novel anthraquinone-based sulfonamide derivatives (**ANS**). In this green strategy (Umpolung strategy), the nature of **DAA** is changed from a nucleophile to an electrophile, simply by capturing its electrons through an electrode. With this strategy, we succeeded in synthesizing unique sulfonamides (**ANS**) *via* a simple method in a divided cell, with both controlled potential and constant current methods, on the surface of a graphite electrode in a water/acetonitrile mixture at room temperature and without using a catalyst, in good yield.

Results and discussion

General studies

The **DAA** has an interesting structure. While its central ring is a reducible quinone ring, its diamine ring can be independently oxidized. Fig. 2 shows the cyclic voltammogram of **DAA** in water (acetate buffer, pH = 5.0, c = 0.2 M)/acetonitrile (40/60 v/v) mixture, which confirms what was previously reported. When the potential is scanned from −0.1 to −1.0 V, the voltammogram shows a well-defined cathodic peak (C_0) at −0.73 V *vs.* SCE. This peak is related to the two-electron reduction of the quinone ring to its diol form (**DAA$_R$**) (Scheme 1). In such a situation, the peak's counterpart (A_0) appears in the reverse scan at −0.65 V. The peak-to-peak separation of the A_0/C_0 redox peaks is 80 mV at 100 mV s^{-1}, indicating a quasi-reversible electrochemical process. When the potential scan is initially performed in the anodic direction, the voltammogram shows an independent anodic peak (A_1) at a potential of 0.56 V, which corresponds to the two-electron oxidation of the *para*-diaminobenzene ring to the corresponding quinonediimine (**DAA$_O$**).

Under these conditions, by reversing the direction of the potential sweep, the cathode peak (C_1) associated with peak A_1 appears at a potential of 0.49 V. The peak-to-peak separation for the A_1/C_1 redox peaks is 70 mV at 100 mV s^{-1}, indicating a quasi-reversible electrochemical process. Notably, the peak current ratio of C_1 to A_1 (I_{pC1}/I_{pA1}) is smaller than one and decreases as the scan rate decreases. This fact indicates the high

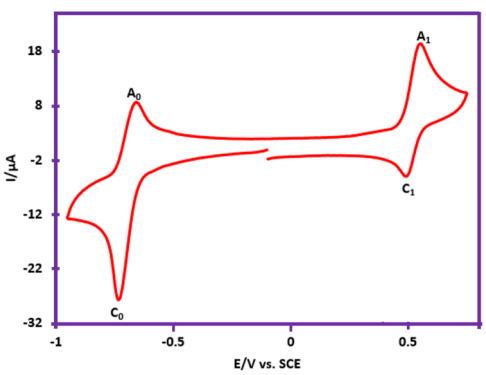

Fig. 2 Cyclic voltammogram of **DAA** (1 mM) in water (acetate buffer, pH = 5.0, c = 0.2 M)/acetonitrile (40/60 v/v) mixture at 100 mV s^{-1} at room temperature. Working electrode: glassy carbon.

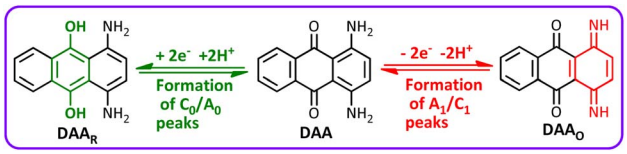

Scheme 1 The reduction and oxidation pathways of **DAA**.

reactivity of **DAA$_O$** and its participation in reactions such as dimerization/polymerization,[3,13] hydrolysis,[14] or ring opening.[15] Moreover, the peak current ratio of C_0 to A_0 (I_{pC0}/I_{pA0}) remains constant with increasing scan rate, indicating the stability of the anthraquinone structure on the voltammetric time scale.[16]

Electrochemical oxidation of DAA in the presence of arylsulfinic acids

The results showed that electrochemically produced **DAA$_O$** is a reactive intermediate and, even in the absence of conventional nucleophiles, can react with the parent **DAA** molecule to form dimers or react with water and be hydrolyzed. In this section, we examine the oxidation mechanism of **DAA** in the presence of a strong nucleophile such as benzenesulfinic acid. Fig. 3, part I, shows the cyclic voltammograms of **DAA** in the absence and presence of benzenesulfinic acid (**SUL1**) to investigate the reactivity of **DAA$_O$** with benzenesulfinic acid. In the presence of **SUL1**, the C_1 peak current decreases, and the extent of this decrease increases with increasing **SUL1** concentration; thus, when the **SUL1** concentration reaches 2 mM, no trace of peak C_1 is observed. Notably, the shift of the A_1 peak potential toward more positive potentials is due to fouling of the electrode surface by the product resulting from the reaction of **DAA$_O$** with **SUL1**, which reduces the efficiency of the electrode.

Increasing the potential scan rate has the opposite effect as increasing the **SUL1** concentration, such that the peak current ratio I_{pC1}/I_{pA1} increases with the potential scan rate. Fig. 3, part

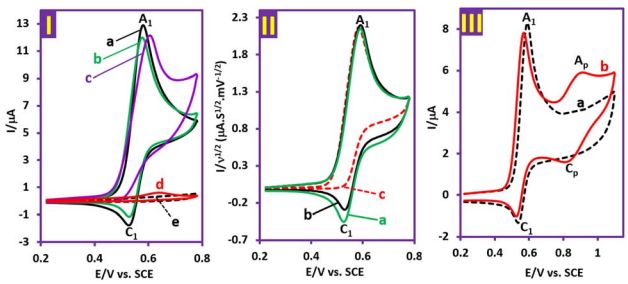

Fig. 3 Part I. Cyclic voltammograms of **DAA** (1.0 mM): (a) in the absence of **SUL1**. (b) In the presence of 1.0 mM **SUL1**. (c) In the presence of 2.0 mM **SUL1**. (d) Cyclic voltammogram of **SUL1** (1.0 mM) in the absence of **DAA** and (e) background electrolyte at a scan rate of 25 mV s^{-1}. Part II. Normalized cyclic voltammograms of **DAA** (1.0 mM) in the presence of 1.0 mM **SUL1** at different scan rates: (a) 100, (b) 50, and (c) 10 mV s^{-1}. Part III. Cyclic voltammograms of **DAA** (1.0 mM). (a) In the absence of **SUL1**. (b) In the presence of 1.0 mM **SUL1** at a scan rate of 25 mV s^{-1}. Solvent: a mixture of water (acetate buffer, pH = 5.0, c = 0.2 M)/acetonitrile (40/60 v/v) at room temperature. Working electrode: glassy carbon.

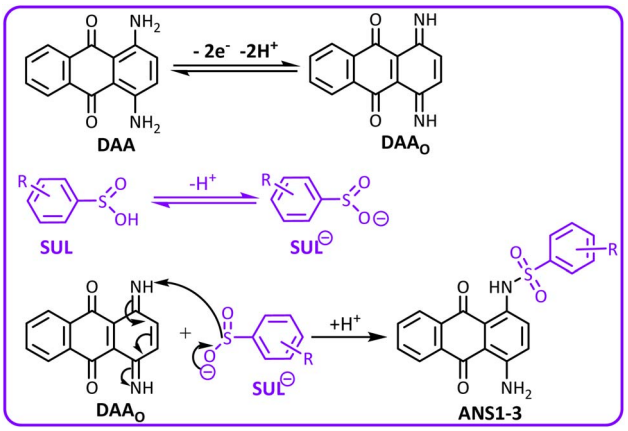

Scheme 2 Electrochemical oxidation pathway of DAA in the presence of SUL.

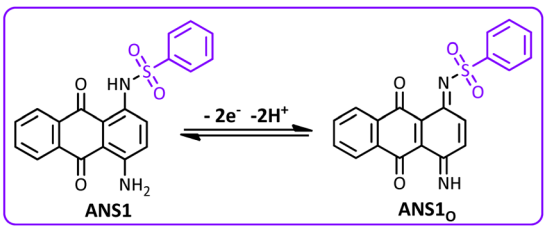

Scheme 3 Redox reactions associated with the A_p and C_p peaks.

II, which shows normalized voltammograms of **DAA** in the presence of **SUL1**, clearly shows the effect of increasing the scan rate on the voltammogram shape. Notably, normalization is achieved by dividing the current (μA) by the square root of the scan rate (mV s^{-1}).

Fig. 3, part III, CVb, shows the cyclic voltammogram of **DAA** in the presence of **SUL1**, in which the anodic switching potential has been extended to 1.1 V, and compares it with the cyclic voltammogram of **DAA** in the absence of **SUL1**. In this case, a new pair of peaks (A_p and C_p) appears at more positive potentials, which could be related to the redox reaction of the product formed at the electrode surface. These results confirm the reaction between **DAA$_O$** and **SUL1** and indicate that the reaction of **DAA$_O$** with **SUL1** is faster than other possible reactions, such as hydrolysis, dimerization, and ring opening. Based on the voltammetric data as well as the spectroscopic results of the synthesized product, the following mechanism (Scheme 2) is proposed for the oxidation of **DAA** in the presence of **SUL**. Further oxidation of the product (**ANS**) does not occur under the conditions used because the oxidation of the product is more difficult than that of the starting material (**DAA**), due to the presence of the electron-withdrawing benzenesulfinyl group and the insolubility of the product in the electrolysis solution.

As shown in Fig. 3, part III, the redox reaction associated with peaks A_p and C_p is shown in Scheme 3. The presence of the electron-withdrawing benzenesulfinyl group in the **ANS1** structure causes its oxidation to occur at more positive potentials than **DAA** does.

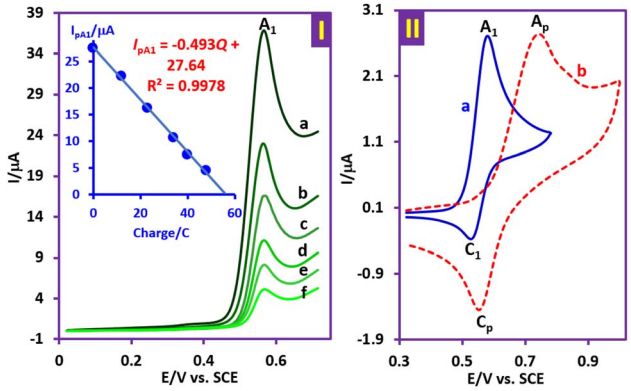

Fig. 4 Part I: linear sweep voltammograms of DAA (0.25 mmol) in the presence of SUL1 (0.25 mmol) during controlled-potential coulometry at 0.70 V *vs.* SCE. (a): 0 C, (b) 12 C, (c) 23 C, (d) 34 C, (e) 34 C and (f) 48 C. (inset): Variations in the A_1 peak current (I_{pA1}) *versus* the charge consumption. Part II: (a) cyclic voltammogram of DAA and (b) cyclic voltammogram of a saturated solution of the product (**ANS1**). The current of CVa decreases by approximately 80% compared with that of CVb. Scan rate of 25 mV s^{-1}. Solvent: a mixture of water (acetate buffer, pH = 5.0, c = 0.2 M)/acetonitrile (40/60 v/v) at room temperature. Working electrode: glassy carbon.

Controlled-potential synthesis

Controlled potential coulometry was performed to determine the number of electrons exchanged during **DAA** oxidation in the presence of **SUL1**, and the coulometric progress was followed *via* linear sweep voltammetry (Fig. 4, part I). The experiment was conducted in a two-compartment cell with a water (acetate buffer, pH = 5.0, c = 0.2 M)/acetonitrile (40/60 v/v) mixture.

According to the coulometric results and the line equation obtained *via* coulometry (Fig. 4, part I, inset), the number of electrons consumed per **DAA** molecule is 2.3, which is consistent with what was reported in Scheme 2 (n = 2) for the oxidation of **DAA** in the presence of **SUL1**.

After isolation and purification of the product (**ANS1**), the cyclic voltammogram of its saturated solution was recorded (Fig. 4, part II, CVb) and compared with the cyclic voltammogram of **DAA** (Fig. 4, part II, CVa). Notably, the CVa currents were reduced by approximately 80% for better comparison. Two important points can be drawn from this comparison: (1) the oxidation of the product (**ANS1**) has become more difficult than that of the starting material (**DAA**). This change can be explained by the addition of the electron-withdrawing benzenesulfinyl group to the amine group. (2) The peak current ratio of **ANS1** (I_{pCp}/I_{pAp}) is greater than that of the starting material (I_{pC1}/I_{pA1}). This indicates that the participation of the oxidized form of the product (**ANS1$_O$**) in side reactions, such as dimerization, is less than that of **DAA$_O$** due to the addition of the benzenesulfinyl group to the amine group. The addition of a benzenesulfinyl group to the nitrogen atom eliminates (or greatly reduces) the nucleophilicity of the amine group and therefore slows down the rate of dimerization resulting from the reaction of **ANS1** with **ANS1$_O$**.

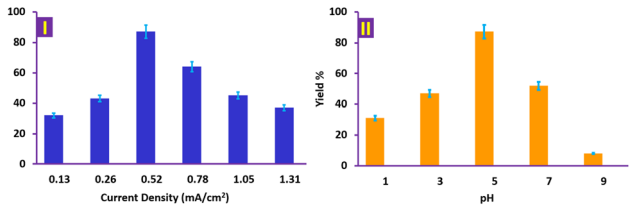

Fig. 5 Part I: effect of current density on the yield of **ANS1**. **DAA**: 0.5 mmol. **SUL1**: 1.0 mmol. Charge: 60 coulombs. Solvent: a mixture of water (acetate buffer, pH = 5.0, c = 0.2 M)/acetonitrile (40/60 v/v) at room temperature. Part II: effect of pH on the yield of **ANS1** at 0.52 mA cm^{-2}. The other conditions are the same as those in part I. Values represent means ± SD of three experiments.

Galvanostatic synthesis

In this section, the efficiency of the constant current method in the synthesis of **ANS** compounds was investigated due to its greater simplicity. However, it should be noted that the efficiency of this method is strongly affected by parameters such as the applied current density and the amount of electricity consumed. Based on the results obtained in the previous section, the amount of electricity consumed in the experiments is considered to be 60 coulombs (1.24 F mol^{-1}). To optimize the current density, current densities of 0.13, 0.26, 0.52, 0.78, 1.05, and 1.31 mA cm^{-2} were applied to the cell, and the **ANS1** synthesis yield was investigated by keeping the other parameters constant. The results of these experiments are shown in Fig. 5, part I. The results show that the optimal current density for **ANS1** synthesis is 0.52 mA cm^{-2}. At lower current densities, owing to the lower overvoltage, **DAA** oxidation and, consequently, $\mathbf{DAA_O}$ formation occur at a slower rate, which causes the **DAA** to $\mathbf{DAA_O}$ concentration ratio at the electrode surface to be high. Under such conditions, the competition between the dimerization reaction and the sulfonylation reaction is high, and therefore, the yield of **ANS1** decreases. On the other hand, since in this optimization, the amount of electricity is kept constant (60 coulombs), at current densities higher than 0.52 mA cm^{-2}, the possibility of selective oxidation of **DAA** decreases. In other words, as the current density increases, the current efficiency decreases and, consequently, the yield also decreases. Here, side reactions that can occur and reduce the current efficiency include: over-oxidation of **ANS1**, oxidation of the nucleophile, solvent, or supporting electrolyte.

For pH optimization, electrolysis was performed at 0.52 mA cm^{-2} at different pH values (1.0, 3.0, 5.0, 7.0, and 9.0), and the results are shown in Fig. 5, part II. The results show that the optimal pH value for **ANS1** synthesis is 5.0. The decrease in yield at more acidic pH values could be due to protonation of the nucleophile, leading to its inactivation as a nucleophile. On the other hand, an acidic environment causes the protonation of **DAA**, making it more difficult to oxidize. This condition allows other side oxidation processes to participate in the oxidation process. At pH values higher than 5.0, the occurrence of side reactions such as dimerization reactions, hydroxylation, or overoxidation of **ANS1** causes a decrease in yield. **DAA** dimerization can be reduced by oxidation in more dilute solutions.

Conclusions

The idea of synthesizing **ANS** derivatives arose when researchers discovered that anthraquinone-based benzenesulfonamide derivatives had significant pharmacological properties. Therefore, we decided to synthesize new sulfonamides containing an anthraquinone moiety. We developed a simple and practical one-pot electrochemical method to achieve this goal. In this method, we took advantage of the change in the nature of **DAA** from a nucleophile to an electrophile, by capturing its electrons *via* an electrode (Umpolung strategy). Detailed voltammetric studies revealed that when **DAA** is oxidized, a reactive intermediate ($\mathbf{DAA_O}$) is formed that can participate in various reactions. However, if strong nucleophiles, such as arylsulfinic acids, are present in the presence of $\mathbf{DAA_O}$, $\mathbf{DAA_O}$ will undergo a chemical reaction with them and be converted to the desired product. This result was exactly what we needed, and on the basis of our data, we performed electrolysis on a preparative scale and succeeded in synthesizing the desired products. In this work, to simplify and generalize the method, in addition to the controlled-potential synthesis method, the constant current method was also used, and the parameters affecting it were optimized. The results show that the highest yield at pH 5.0 (aqueous acetate buffer, pH = 5.0, c = 0.2 M)/acetonitrile (40/60 v/v) is achieved by applying a current density of 0.52 mA cm^{-2} in a divided cell equipped with graphite anodes and stainless steel cathodes.

Experimental section

Reagents and apparatus

1,4-Diaminoanthraquinone (**DAA**) (catalogue number 842128, for synthesis-grade), benzenesulfinic acid sodium salt (98%) (**SUL1**) (catalogue number 123579), 4-toluenesulfinic acid sodium salt (95%) (**SUL2**) (catalogue number 455652), acetonitrile (catalogue number 100030, gradient grade), ethyl acetate (catalogue number 109623, for analysis-grade), *n*-hexane (98.50%) (catalogue number 104374), sodium acetate (catalogue number 106264, ACS reagent), and hydrochloric acid (catalogue number 109060, c(HCl) = 0.1 mol l^{-1} (0.1 N)) were purchased from Merck and Sigma-Aldrich and were used without purification.

The cyclic voltammetry and linear sweep voltammetry experiments were performed using an Autolab PGSTAT 20 potentiostat/galvanostat. Cyclic voltammograms were recorded at 25 °C *via* a three-electrode system with a 1.8 mm-diameter (2.5 mm^2 area) glassy carbon disc as the working electrode, a stainless-steel wire as the counter electrode, and an Ag/AgCl reference electrode (3 M KCl). All electrodes were manufactured by Azar Electrode Company (Iran). The glassy carbon electrode was polished with alumina slurry.

To record linear sweep voltammograms during coulometry, first, the coulometry was stopped after consuming a certain amount of electricity, and voltammetry was performed after placing the electrodes introduced for voltammetry.

For electrosynthesis under constant current conditions, a Dazheng PS-303D power supply was used, and for

electrosynthesis under controlled potential, a BEHPAJOOH-C2056 potentiostat was used. The syntheses were carried out in a divided cell (100 mL) equipped with a magnetic stirrer, containing four graphite rods (each 4 cm long and 1 cm in diameter) (total anode surface area: 53.4 cm^2) as anodes and a stainless-steel rod as the cathode. The cathode is placed in the cathodic compartment. The cathodic compartment consists of a glass tube (10 mm diameter), closed at one end by a medium-porosity glass frit and containing a mixture of acetate buffer (pH = 5.0, c = 0.2 M)/acetonitrile (40/60, v/v). The cathodic compartment is placed in the center, and the graphite electrodes are placed at equal distances at the four corners of a square to distribute the potential evenly across all the anodes. Acetonitrile was used as a cosolvent to increase its solubility because of the low solubility of **DAA** in water. The ohmic resistance between the anode and the cathode in this configuration was about 400 Ohm.

Synthesis of 2-chlorobenzenesulfinic acid (SUL3)

2-Chlorobenzenesulfinic acid (**SUL3**) was synthesized in our laboratory according to the literature[17] as described in the patent.[18] Sodium sulfite (8.96 g, 71.1 mmol) and 2-chlorobenzenesulfonyl chloride (5 g, 23.7 mmol) were dissolved in 50 mL of water. The mixture was then heated at 80 °C for 5 h, and the completion of the reaction was checked by TLC. After the reaction mixture was cooled to room temperature, it was extracted with dichloromethane (2 × 50 mL). Then, the pH of the aqueous layer was adjusted to 2–3 by adding 6 M HCl, which resulted in the formation of a white precipitate. The precipitate was filtered and washed with water 2–3 times to give a white, needle-shaped product (3.68 g, 87.9% yield).

General approach for the synthesis of ANS1–ANS3

A mixture of acetate buffer (pH = 5.0, c = 0.2 M)/acetonitrile (40/60, v/v) (70 mL) containing **DAA** (0.5 mmol, 0.119 g) and **SUL** (1.0 mmol) was electrolyzed in a divided cell equipped with a graphite anode and a stainless-steel rod cathode at 0.60 V *vs.* SCE at room temperature. Electrolysis was terminated when the current decreased by more than 95% (after about 2.5 h). At the end of electrolysis, the solution was concentrated using a rotary evaporator and placed in the refrigerator overnight. The precipitated solid was collected by filtration and washed several times with water. After drying at room temperature for 24 h under ambient pressure, the yield was determined and the product was further purified by thin-layer chromatography on silica gel (50 : 50 ethyl acetate/*n*-hexane). The products (**ANSs**) were characterized by IR, ^{1}H NMR, ^{13}C NMR, and mass spectrometry. In the synthesis of products by the constant current method, a current density of 0.52 mA cm^{-2} is applied to the working electrode (anode), and electrolysis is performed until 60 coulombs of electricity pass through. It should be noted that other conditions are similar to the synthesis by the controlled potential method.

Characteristics of the products

***N*-(4-Amino-9,10-dioxo-9,10-dihydroanthracen-1-yl) benzenesulfon amide (ANS1) ($C_{20}H_{14}N_2O_4S$).**

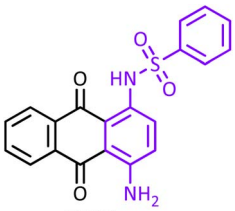

ANS1

Crimson precipitate (0.165 g, yield 87%), Mp. 293–295 °C (dec), ^{1}H NMR δ ppm (500 MHz, $CDCl_3$): 4.35 (broad, 2H, NH), 6.61 (t, 3H, aromatic), 6.73 (d, J = 10 Hz, 2H, aromatic), 7.16–7.20 (m, 6H, aromatic), 7.28 (broad, ~1H, NH). ^{13}C NMR: δ ppm (125 MHz, $CDCl_3$): 109.7, 117.6, 126.4, 127.0, 127.3, 128.0, 129.8, 129.9, 133.6, 134.1, 182.9, 185.8. IR (KBr) (cm^1): 3441, 3301, 2823, 1731, 1633, 1579, 1542, 1457, 1366, 1269, 1158, 1089, 971, 727, 571. MS (m/z) (EI, 70 EV) (relative intensity): 77 (70), 127 (50), 182 (60), 209 (62), 237 (100), 378 (M, 70).

***N*-(4-Amino-9,10-dioxo-9,10-dihydroanthracen-1-yl)-4-methylbenzenesulfonamide (ANS2) ($C_{21}H_{16}N_2O_4S$).**

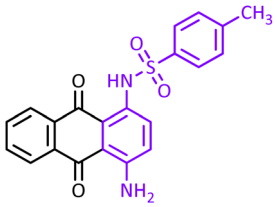

ANS2

Crimson precipitate (0.161 g, yield 82%), Mp. 285–288 °C (dec), ^{1}H NMR δ ppm (500 MHz, $CDCl_3$): 2.24 (s, 3H, CH_3), 7.26–7.31 (m, 3H, aromatic), 7.69 (d, J = 10 Hz, 2H, aromatic), 7.78–7.92 (m, 3H, aromatic), 8.11 (d, J = 10 Hz, 2H, aromatic), 12.25 (s, 1H, NH). ^{13}C NMR: δ ppm (125 MHz, $CDCl_3$): 21.4, 109.6, 117.5, 126.5, 127.0, 127.3, 128.1, 130.1, 132.1, 132.9, 133.8, 135.2, 136.3, 144.6, 149.8, 182.9, 186.9. IR (KBr) (cm^1): 3447, 3307, 3070, 2919, 2953, 2853, 1685, 1636, 1592, 1542, 1470, 1370, 1268, 1158, 1088, 971, 914, 881, 814, 714, 656, 547. MS (m/z) (EI, 70 EV) (relative intensity): 65 (40), 91 (100), 155 (20), 237 (80), 391 (M–1, 30).

***N*-(4-Amino-9,10-dioxo-9,10-dihydroanthracen-1-yl)-2-chlorobenzene sulfonamide (ANS3) ($C_{20}H_{13}ClN_2O_4S$).**

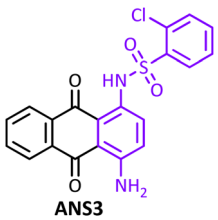

ANS3

Crimson color (0.157 g, yield 76%), Mp. 310–312 °C (dec), ^{1}H NMR δ ppm (500 MHz, DMSO-d_6): 7.30 (d, J = 10 Hz, 1H,

aromatic), 7.58 (d, $J = 10$ Hz, 2H, aromatic), 7.72 (d, $J = 10$ Hz, 1H, aromatic), 7.80–7.90 (m, 4H, aromatic), 8.11–8.15 (m (2d), 2H, aromatic), 12.2 (broad, 1H, NH). ^{13}C NMR: δ ppm (125 MHz, DMSO-d_6): 109.8, 126.6, 127.0, 128.1, 129.3, 130.1, 133.8, 134.1, 182.8, 196.2. IR (KBr) (cm^1): 3482, 3317, 2920, 2850, 1636, 1591, 1574, 1538, 1435, 1434, 1361, 1343, 1278, 1157, 1092, 970, 915, 829, 728, 609, 588. MS (m/z) (EI, 70 EV) (relative intensity): 75 (30), 111 (40), 182 (50), 209 (62), 237 (100), 412 (M, 50).

Ethical statement

This article does not contain any studies with animals per formed by any of the authors.

Author contributions

Davood Nematollahi: supervision, project administration, resources, writing – review & editing, conceptualization. Niloofar Mohamadighader: investigation, project administration, data curation. Faezeh Zivari-Moshfegh: investigation, project administration, writing – original draft.

Conflicts of interest

There are no conflicts to declare.

Data availability

The data that supports the findings of this study are available in the supplementary information (SI) of this article. Supplementary information: FT-IR, ^{1}H NMR, ^{13}C NMR and MS spectra of **SUL1–SUL3**. See DOI: https://doi.org/10.1039/d6ra00036c.

Acknowledgements

We acknowledge the Bu-Ali Sina University Research Council and the Center of Excellence in Development of environmentally Friendly Methods for Chemical Synthesis (CEDEFMCS) for their support of this work.

Notes and references

1 G. Diaz-Munoz, I. L. Miranda, S. K. Sartori, D. C. De Rezende and M. A. Diaz, *Anthraquinones: an Overview, Studies in Natural Products Chemistry*, ed. B. T. S. Atta-ur-Rahman, Elsevier, 2018, vol. 58, pp. 313–338.

2 R. Goyal, S. Aggarwal, V. Saini, R. K. Gautam and S. Ahmed, Biobased Materials in Nutraceuticals, *Advanced Applications of Biobased Materials*, 2023, pp. 245–262.

3 F. Yakuphanoglu and B. F. Şenkal, A hybrid *p*-Si/poly (1,4-diaminoanthraquinone) photoconductive diode for optical sensor applications, *Synth. Met.*, 2009, **159**, 311–314.

4 M. E. Campbell and J. Mueller, Synthesis of 1,4-diaminoanthraquinones for the purification of lactate dehydrogenase, *FASEB J.*, 2018, **32**, 797–799.

5 A. E. Weber, R. J. Mathvink, L. Perkins, J. E. Hutchins, M. R. Candelore, L. Tota, C. D. Strader, M. J. Wyvratt and M. H. Fisher, Potent, selective benzenesulfonamide agonists of the human beta 3 adrenergic receptor, *Bioorg. Med. Chem. Lett.*, 1998, **8**, 1101–1106.

6 E. R. Parmee, H. O. Ok, M. R. Candelore, L. Tota, L. Deng, C. D. Strader, M. J. Wyvratt, M. H. Fisher and A. E. Weber, Discovery of L-755,507: A subnanomolar human beta 3 adrenergic receptor agonist, *Bioorg. Med. Chem. Lett.*, 1998, **8**, 1107–1112.

7 T. Maruyama, K. Onda, M. Hayakawa, T. Matsui, T. Takasu and M. Ohta, Discovery of novel acetanilide derivatives as potent and selective β3-adreergic receptor agonists, *Eur. J. Med. Chem.*, 2009, **44**, 2533–2543.

8 X. Zheng, H. Oda, K. Takamatsu, Y. Sugimoto, A. Tai, E. Akaho, H. I. Ali, T. Oshiki, H. Kakuta and K. Sasaki, Analgesic agents without gastric damage: Design and synthesis of structurally simple benzenesulfonanilide-type cyclooxygenase-1-selective inhibitors, *Bioorg. Med. Chem.*, 2007, **15**, 1014–1021.

9 Y. Rew, M. DeGraffenreid, X. He, J. C. Jaen, D. L. McMinn, D. Sun, H. Tu, S. Ursu and J. P. Powers, Discovery and optimization of benzenesulfonanilide derivatives as a novel class of 11β-HSD1 inhibitors, *Bioorg. Med. Chem. Lett.*, 2012, **22**, 3786–3790.

10 A. Yamada, Y. Kazui, H. Yoshioka, A. Tanatani, S. Mori, H. Kagechika and S. Fujii, Development of *N*-(4-phenoxyphenyl) benzenesulfonamide derivatives as novel nonsteroidal progesterone receptor antagonists, *ACS Med. Chem. Lett.*, 2016, **7**, 1028–1033.

11 V. Ouellette, A. C. Alvarez, C. Bouzriba, G. Hamel-Côté and S. Fortin, 4-(3-Alkyl-2-oxoimidazolidin-1-yl)-*N*-phenylbenzenesulfonamide salts: Novel hydrosoluble prodrugs of antimitotics selectively bioactivated by the cytochrome P450 1A1 in breast cancer cells, *Bioorg. Chem.*, 2023, **140**, 106820.

12 S. Wu, X. Zhou, F. Li, W. Sun, Q. Zheng and D. Liang, Novel anthraquinone-based benzenesulfonamide derivatives and their analogs as potent human carbonic anhydrase inhibitors with antitumor activity: Synthesis, biological evaluation, and in silico analysis, *Int. J. Mol. Sci.*, 2024, **25**, 3348.

13 M. Jamshidi, D. Nematollahi and H. Amiri Rudbari, Electrochemical oxidation of p-aminoacetanilide in aqueous solutions: A green electrochemical protocol for the synthesis of azo dyes, *J. Electrochem. Soc.*, 2016, **163**, G145–G152.

14 A. Maleki and D. Nematollahi, Mechanism diversity in anodic oxidation of *N*,*N*-dimethyl-*p*-phenylenediamine by varying pH, *J. Electroanal. Chem.*, 2013, **704**, 75–79.

15 D. Nematollahi and F. Varmaghani, Kinetic study of 4-nitrocatechol oxidation using digital simulation of cyclic voltammograms, *J. Iran. Chem. Soc.*, 2011, **8**, 803–810.

16 D. Nematollahi, S. Alizadeh, A. Amani and S. Khazalpour, *Practical Aspects of Electroorganic Synthesis*, Elsevier, 2024.

17 L. K. Liu, Y. Chi and K. Y. Jen, Copper-catalyzed additions of sulfonyl iodides to simple and cyclic alkenes, *J. Org. Chem.*, 1980, **45**, 406–410.

18 H. U. Tianliang, Q. Meng, S. Zhou, F. Tao, Shandong University, assignee. Digital twin intelligent edge terminal and operation method therefor. *US. Pat.*, 12,360,518. 2025.